ARKIV FÖR FYSIK Band 16 nr 46

Communicated 28 October 1959 by M. Siegbahn and O. Klein

Shell model calculations in the lead region with a diffuse nuclear potential

By J. Blomqvist and S. Wahlborn

With 2 figures in the text

ABSTRACT

With the use of a diffuse potential of the Woods-Saxon type, including a spin-orbit interaction, numerical solution of the single nucleon Schrödinger equation is performed, with values of the potential parameters appropriate to the lead region. Single particle energies and radial wave functions are obtained for the orbitals in the major shells adjacent to $Z = 82$ and $N = 126$, and the changes of the energy eigenvalues with the parameters are estimated. Pairing energy corrections are introduced. The possible occurrence of quadrupole oscillation states is considered, and the corresponding collective corrections to the single particle states are applied. The perturbed energies are compared with the level schemes of the four nuclei, which differ from the double-magic Pb^{208} with one nucleon, and some suggestions and predictions are made.

1. Introduction

The use of a nuclear potential with a diffuse surface in shell model calculations has been necessitated by experience [1]. In the optical model analysis of cross sections for the elastic scattering of nucleons from nuclei, a potential of the form

$$V(r) = -V_0[1 + \exp(r - R)/a]^{-1}$$

introduced by Woods and Saxon [2], has often been used [3, 4]. Calculations of bound-state energies with such a potential plus a spin-orbit interaction with the radial dependence

$$r^{-1} dV/dr$$

were first performed by Ross *et al.* [5]. Recently, Sliv and Volchok [6] have studied the nuclear potential parameters with the same assumptions. Similar calculations, though with a somewhat different potential form, have been performed by, among others, Bleuler and collaborators [7].

One of the main objects of the earlier investigations has been to obtain a proper choice of the potential parameters common to the whole periodic system. A more detailed analysis for some specific regions, where the shell model is expected to hold, might be of interest. In the present work, the single particle states in the region around the double-magic nucleus Pb^{208} have been investigated. Pairing energies and effects due to collective motion have been taken into account, causing corrections to the single particle states, and comparison has been made with low energy levels of the four nuclei Pb^{208} plus or minus one nucleon. The principal aim has, thus, been twofold. 1) To obtain the single particle energies, for use in other investigations, and the radial wave functions, designed for the calculation of various matrix elements. 2) To get a simple phenomenological theory of the low-lying states of the nuclei Pb^{209}, Pb^{207}, Bi^{209}, and Tl^{207}.

2. The nuclear potential and the eigenstates

2.1. *The potential and the eigenvalue problem*

According to the model applied, the interaction of a single nucleon with the residual nucleus can be represented by three contributions to the Hamiltonian: A spin-independent central nuclear potential, a spin-orbit coupling term, and, in the case of a proton, a repulsive electrostatic potential, here referred to as the Coulomb-term. We assume the following forms:

a) The central nuclear potential

$$V(r) = -\frac{V_0}{1+\exp\dfrac{r-R}{a}} = -V_0\,\xi(r). \tag{1}$$

$V_0 > 0$ is the depth of the potential and R its radius. With $R = r_0 A^{1/3}$, r_0 is approximately constant over the whole periodic system. $2a$ is a measure of the depth of the surface.

b) The spin-orbit term

$$-\lambda\,\frac{\lambda_c^2}{2}\,\frac{1}{r}\,\frac{dV}{dr}\,(\bar{s}\cdot\bar{l}). \tag{2}$$

λ is a positive dimensionless parameter, characterizing the strength of the coupling. $\lambda_c = \hbar/Mc$ is the reduced Compton wave-length of the nucleon. The angular momentum operators $\bar{s}$ and $\bar{l}$ are given in units of $\hbar$.

c) The Coulomb term

$$(Z-1)\,\frac{e^2}{r}\,\zeta(r), \tag{3}$$

where Z is the proton number and $\zeta(r)$ is chosen to correspond to a uniform charge distribution within the radius R,

$$\zeta_p(r) = \begin{cases} \dfrac{3}{2}\dfrac{r}{R} - \dfrac{1}{2}\left(\dfrac{r}{R}\right)^3, & r \leqslant R, \\ 1, & r \geqslant R, \end{cases} \tag{3a}$$

$$\zeta_n(r) = 0.$$

After elimination of the angular and spin dependence in the single particle Schrödinger equation, there remains the radial wave equation

$$\left\{-\frac{\hbar^2}{2M}\left[\frac{1}{r^2}\frac{d}{dr}\left(r^2\frac{d}{dr}\right)-\frac{l(l+1)}{r^2}\right]-\right.$$
$$-V_0\left[\xi(r)-\lambda\frac{\lambda_c^2}{2}f(l,j)\frac{1}{r}\frac{d\xi(r)}{dr}\right]+$$
$$\left.+(Z-1)\frac{e^2}{r}\zeta(r)\right\}R_{nlj}(r)=E_{nlj}R_{nlj}(r). \tag{4}$$

$f(l, j)$ is the eigenvalue of the operator $(\bar{s}\cdot\bar{l})$, i.e.

$$f(l,j)=\begin{cases}\frac{1}{2}l & \text{for } j=l+1/2,\\ -\frac{1}{2}(l+1) & \text{for } j=l-1/2,\end{cases} \tag{5}$$

and n is the usual [1] radial quantum number ($n-1$ equal to the number of zeros of $R_{nlj}(r)$ for $0<r<\infty$).

After insertion of the function

$$y_{nlj}(r)=r\,R_{nlj}(r) \tag{6}$$

and of numerical values for the constants (units: MeV and 10^{-13} cm), the equation reads

$$y''(r)-\frac{l(l+1)}{r^2}y(r)+0.04823\left\{E+\right.$$
$$\left.+V_0\left[\xi(r)+0.02209\,\lambda f(l,j)\frac{-\xi'(r)}{r}\right]\right\}y(r)-$$
$$-0.06939(Z-1)\frac{\zeta(r)}{r}y(r)=0. \tag{7}$$

The subscripts nlj have been omitted for simplicity. The boundary and normalization conditions are

$$y(0)=y(\infty)=0,\quad \int_0^\infty[y(r)]^2dr=1. \tag{8}$$

We put $Z-1=82$ in the following.

The unphysical singularity of $\xi'(r)/r$ for $r=0$ is removed by setting $\xi(r)=1$ in a small region $r\leqslant b\ll R$. The appropriate solution $y(r)$ is then proportional to r times a spherical Bessel function for $r\leqslant b$; see equation (A.4) in Appendix A. For the normalization one needs a fairly correct representation of $y(r)$ for large values of r, $r-R\gg a$. The asymptotic form is given in Appendix A

The eigenvalue problem (7), (8) has been treated numerically with the Swedish electronic computer BESK. Given the potential parameters, the eigenvalue E for a state nlj can easily be estimated with sufficient accuracy for the adopted procedure. Equation (7) is then integrated with the method of Runge-Kutta, starting at the point $r = b$ (a suitable choice of b is $0.5 \cdot 10^{-13}$ cm). The following rule holds:

$$(-1)^n y(r) \underset{r\to\infty}{\rightarrow} +\infty \quad \text{if} \quad E > E_{nlj},$$

$$(-1)^n y(r) \underset{r\to\infty}{\rightarrow} -\infty \quad \text{if} \quad E < E_{nlj},$$

where E_{nlj} is the exact eigenvalue. The difference $E - E_{nlj}$ varies smoothly with $y(r)$ at a sufficiently large value of r. These facts furnish a rapidly convergent iterative procedure for getting the eigenvalues very accurately. The asymptotic form of the eigensolution $y(r)$, however, has to be calculated by other means, and the expression (A.6) has been used for this purpose. The "tail" is then fitted to the integrated solution $y(r)$ at a suitable point $r = d$ (d has here generally been chosen as $13 \cdot 10^{-13}$ cm). Finally, the functions $y(r)$ have been normalized according to (8).

2.2. *Parameters and results*

The choice of the nuclear potential parameters is given in the first row of Table 1. They are compared with the values obtained by other authors from shell model calculations [5, 6] and optical model analysis [3, 4].

The number of decimal figures, which we have chosen for our parameters, is such that another decimal would certainly be physically insignificant. The parameters have not been fitted in detail to any specific level data, but have been chosen to fulfil the following approximate conditions, which fix their values fairly well.

(I) The values should be in rough agreement with the results obtained by other authors for the whole periodic system, according to Table 1. We set the limits: $R = (7.6 \pm 0.3) \cdot 10^{-13}$ cm, $V_0^n = 45 \pm 5$ MeV, $V_0^p = 57 \pm 5$ MeV, $a = (0.7 \pm 0.1) \cdot 10^{-13}$ cm, $\lambda = 35 \pm 5$.

Table 1. The potential parameters.

Reference		r_0 10^{-13} cm	R 10^{-13} cm	V_0 MeV		a 10^{-13} cm	λ
				Neutron	Proton		
The present choice for the Pb-region		1.27[1]	*7.52*	*44.0*	*58.0*	*0.67*	*32*
Sliv and Volchok [6]	Pb^{209}	1.3	7.71[1]	42.6	—	0.87[2]	28
	Pb^{207}		7.69[1]	41.8	—	0.71[2]	39
	Bi^{209}		7.71[1]	—	56.9	0.87[2]	25
	Tl^{207}		7.69[1]	—	55.8	0.73[2]	38
Ross *et al.* [5]		1.3	7.70[1]	42.8	56.6	0.69[2]	39.5
Elastic scattering of neutrons [3]		1.25	7.41[1]	50[3]	—	0.65	35[3]
Elastic scattering of protons [4]		1.25	7.41[1]	—	60[3]	0.65	35[3]

[1] Values appropriate to the Pb-region according to the radius law $R = r_0 A^{1/3}$.
[2] $\alpha = a^{-1}$ given in the references.
[3] Rough estimates.

Table 2. The energy eigenvalues.

Neutron states		Proton states	
State $n\,l\,j$	Energy MeV	State $n\,l\,j$	Energy MeV
$3\,d_{3/2}$	-0.604	$3\,p_{1/2}$	Not bound
$2\,g_{7/2}$	-0.669	$2\,f_{5/2}$	,, ,,
$4\,s_{1/2}$	-1.224	$3\,p_{3/2}$	,, ,,
$1\,j_{15/2}$	-1.722	$1\,i_{13/2}$	-2.277
$3\,d_{5/2}$	-1.820	$2\,f_{7/2}$	-2.691
$1\,i_{11/2}$	-2.955	$1\,h_{9/2}$	-3.541
$2\,g_{9/2}$	-3.683	$3\,s_{1/2}$	-7.032
$3\,p_{1/2}$	-7.232	$2\,d_{3/2}$	-7.515
$2\,f_{5/2}$	-7.986	$1\,h_{11/2}$	-8.663
$3\,p_{3/2}$	-8.130	$2\,d_{5/2}$	-9.346
$1\,i_{13/2}$	-8.429	$1\,g_{7/2}$	-11.064
$2\,f_{7/2}$	-10.279		
$1\,h_{9/2}$	-10.797		

(II) The main features of the level scheme of Pb^{207} below 2.5 MeV should be reproduced, as it contains the best known data in the region (see Appendix C). Especially the difference between the energies of the states $p_{1/2}$ (ground state) and $i_{13/2}$ (experimentally 1.63 MeV) gives a sensitive criterion for the choice of λ.

Table 3. The partial derivatives of the energy eigenvalues with respect to the potential parameters.

	State $n\,l\,j$	$\frac{\partial E}{\partial V_0}$	$\frac{\partial E}{\partial R}\,\frac{\text{MeV}}{10^{-13}\text{ cm}}$	$\frac{\partial E}{\partial a}\,\frac{\text{MeV}}{10^{-13}\text{ cm}}$	$\frac{\partial E}{\partial \lambda}$ MeV
Neutron states	$3\,d_{3/2}$	-0.44	-4.9	-3.1	$+0.022$
	$2\,g_{7/2}$	-0.59	-7.1	-0.8	$+0.052$
	$4\,s_{1/2}$	-0.42	-4.3	-3.2	0
	$1\,j_{15/2}$	-0.77	-8.3	$+7.6$	-0.107
	$3\,d_{5/2}$	-0.55	-5.5	-2.5	-0.016
	$1\,i_{11/2}$	-0.73	-9.2	$+7.7$	$+0.086$
	$2\,g_{9/2}$	-0.69	-6.8	$+0.7$	-0.041
	$3\,p_{1/2}$	-0.69	-6.4	-0.1	$+0.019$
	$2\,f_{5/2}$	-0.73	-7.0	$+2.2$	$+0.041$
	$3\,p_{3/2}$	-0.72	-6.2	$+0.3$	-0.009
	$1\,i_{13/2}$	-0.81	-7.3	$+8.0$	-0.084
	$2\,f_{7/2}$	-0.78	-6.4	$+2.8$	-0.031
	$1\,h_{9/2}$	-0.80	-7.8	$+8.5$	$+0.063$
Proton states	$1\,i_{13/2}$	-0.83	-10.0	$+11.3$	-0.109
	$2\,f_{7/2}$	-0.81	-9.3	$+4.5$	-0.039
	$1\,h_{9/2}$	-0.82	-11.0	$+11.9$	$+0.079$
	$3\,s_{1/2}$	-0.83	-8.7	$+4.1$	0
	$2\,d_{3/2}$	-0.84	-9.1	$+5.8$	$+0.034$
	$1\,h_{11/2}$	-0.86	-8.9	$+10.9$	-0.080
	$2\,d_{5/2}$	-0.86	-8.4	$+5.7$	-0.023
	$1\,g_{7/2}$	-0.87	-9.4	$+11.5$	$+0.056$

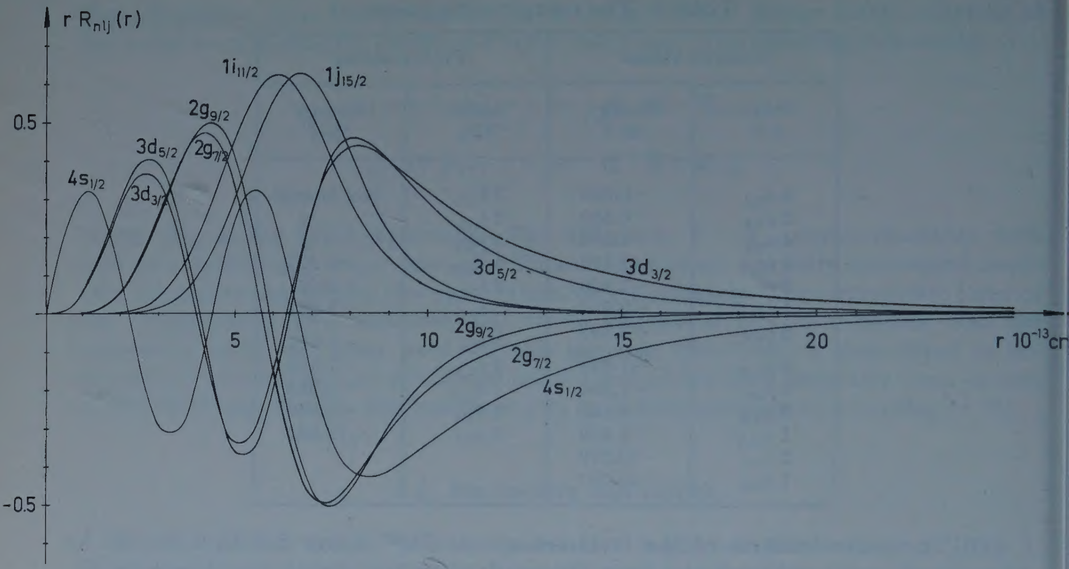

Fig. 1 a.

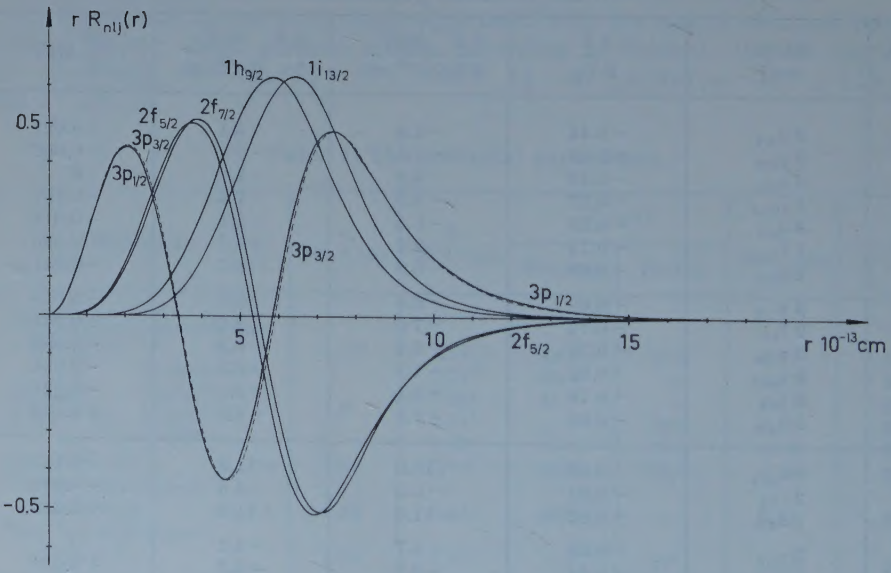

Fig. 1 b.

Fig. 1a and 1b. The normalized function $y_{nlj}(r) = rR_{nlj}(r)$ for neutron states,

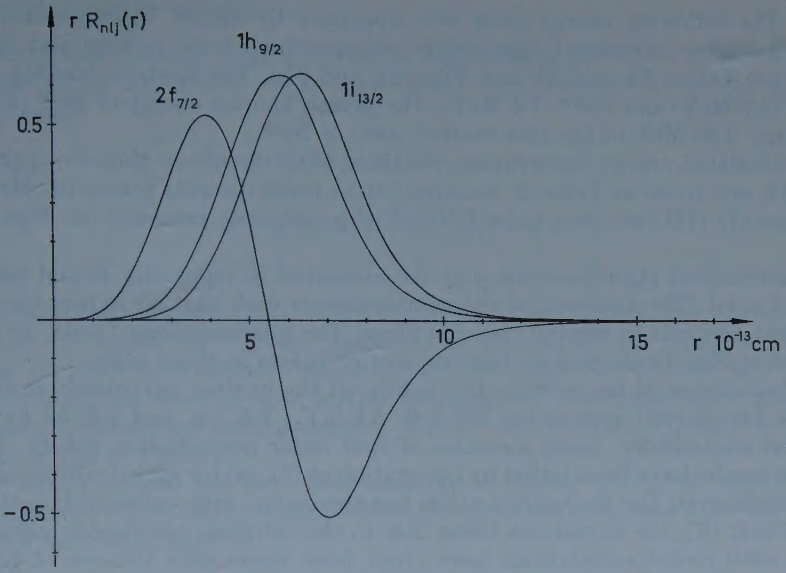

Fig. 1 c.

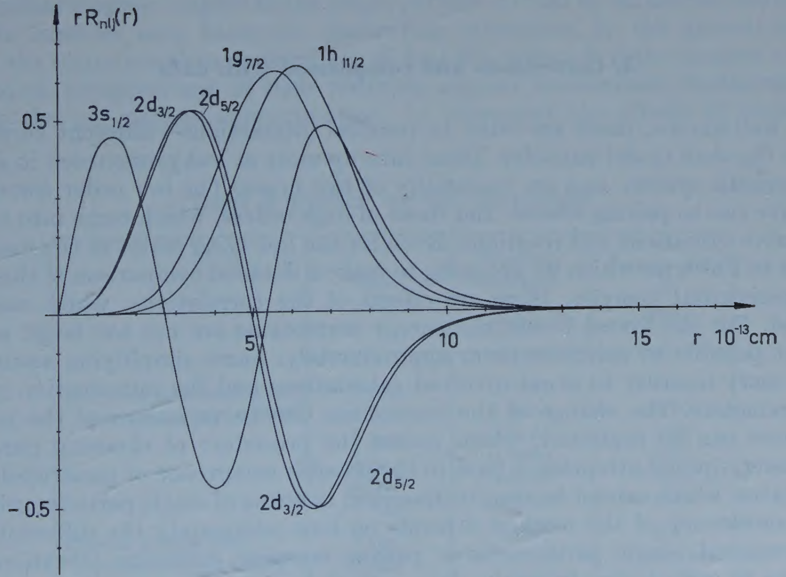

Fig. 1 d.

Fig. 1c and 1d. The normalized function $y_{nlj}(r) = rR_{nlj}(r)$ for proton states.

(III) The following energy data (see Appendix C) should be approximately reproduced by the calculated eigenvalues when corrected for pairing and collective effects (see Tables 5a and 5b and Figs. 2a and 2b): The neutron binding energies of Pb^{209} (3.9 MeV) and Pb^{208} (7.4 MeV). The proton binding energy of Bi^{209} (3.7 MeV). The energy 0.90 MeV of the first excited state of Bi^{209}.

The calculated energy eigenvalues, obtained with the above choice of parameters (Table 1), are given in Table 2, rounded off to three decimal places (in MeV). The conditions (I)–(III) are seen to be fulfilled with sufficient precision (cf. Figs. 2a and 2b).

The normalized eigenfunctions $y(r)$ are tabulated in Appendix B and plotted in Figures 1a–1d. The accuracy of the calculations is such that we expect the error to be at most one unit in the last decimal place. The relatively long "tails" in some of the cases of Fig. 1a depend on the low energy values in these cases.

The dependence of the energy eigenvalues on the nuclear parameters is shown in Table 3. The partial derivatives $\partial E/\partial R$, $\partial E/\partial V_0$, $\partial E/\partial a$, and $\partial E/\partial \lambda$ have been evaluated numerically, using formulas of first order perturbation theory. In some cases the results have been tested by integration of (7), (8) for slightly different values of the parameters. The derivatives are in fair agreement with values obtained by Sliv and Volchok [6], the deviations being due to the different parameter values used.

Since shell model calculations have often been made with the use of harmonic oscillator radial wave functions (cf., for instance, True and Ford [8]), it is of some interest to expand the more physical wave functions, which have been obtained with a diffuse potential, in these oscillator functions. This has not been done in the present work. Sliv and Volchok [6] have investigated this point, and their results should hold essentially unchanged for the functions obtained here.

3. Corrections and comparison with data

As is well-known, there are—due to residual interactions—different correlations between the shell model particles. These turn up more or less pronounced in all parts of the periodic system, and are essentially of two types: The low order correlations, which give rise to pairing effects, and those of high orders, which come into evidence in collective vibrations and rotations. Even for the low-lying states of the four nuclei adjacent to Pb^{208}, for which we are going to make a detailed comparison of theoretical and experimental energies, there are effects of the correlations, which cannot be neglected. For the lowest levels, the energy corrections are not too large, and this makes it possible to calculate them approximately. Some simplifying assumptions are necessary in order to avoid involved calculations and the introduction of many new parameters. The change of the corrections due to variations of the potential parameters can be neglected, which makes the procedure of choosing parameters much easier. Special attention is paid to the possible occurrence of quadrupole vibrational states, which cannot be simply described in terms of single particle excitations.

The consistency of the method depends on how adequately the different effects are represented (single particle states; pairing energies; collective vibrations). One may hope to get a better fit to the data with the corrections applied than with the pure single particle states.

a. *The pairing energy corrections*

The interaction causing pairing effects is here represented by a δ-function. The pairing energy for an orbital nlj is then to the first order given by the diagonal matrix element

$$\delta = -K(2j+1)\,I_{nlj} =$$

$$= -K(2j+1)\int_0^\infty [R_{nlj}(r)]^4\, r^2\, dr. \tag{9}$$

The quantities δ are added as corrections to the single particle energies corresponding to states in the nuclei Pb^{208} *minus* one nucleon. We neglect the possible effects of scattering of pairs between the major shells. The value $K = 6 \cdot 10^{-39}$ MeV $\cdot$ cm^3 is chosen for both the neutron and proton cases, giving reasonable agreement with experimentally estimated pairing energies. The overlap integrals I_{nlj} and the corrections δ are given in Table 4.

As the admixtures to the wave functions due to pairing effects are negligible for our purposes, we will continue to speak of single particle states, even after the pairing corrections have been applied.

b. *The collective corrections*

An odd nucleon or nucleon hole, moving in the field of Pb^{208}, has a polarizing influence on the otherwise spherically symmetric, closed shell nucleus. This is a non-static effect which quantum-mechanically can be described as a collective oscillation of the nuclear surface coupled to the single particle motion by an interaction operator H_{int}. We consider only harmonic quadrupole vibrations. In the general coupling scheme, the states are then denoted $|lj;\, NR;\, JM\rangle$, where N is the number of vibration quanta, phonons, and R their resulting angular momentum. Furthermore, we will use the one-phonon-approximation, i.e. disregard the effects of states with

Table 4. Pairing energy corrections.

	State nlj	Overlap integral I_{nlj} 10^{39} cm^{-3}	Correction δ MeV
Neutron hole states (corresponding to Pb^{207})	$3\,p_{1/2}$	0.0137	-0.16
	$2\,f_{5/2}$	0.0084	-0.30
	$3\,p_{3/2}$	0.0141	-0.34
	$1\,i_{13/2}$	0.0068	-0.57
	$2\,f_{7/2}$	0.0083	-0.40
	$1\,h_{9/2}$	0.0082	-0.49
Proton hole states (corresponding to Tl^{207})	$3\,s_{1/2}$	0.0392	-0.47
	$2\,d_{3/2}$	0.0124	-0.30
	$1\,h_{11/2}$	0.0082	-0.59
	$2\,d_{5/2}$	0.0119	-0.43
	$1\,g_{7/2}$	0.0091	-0.44

Table 5 a. Collective corrections to the single-particle states in the cases Pb^{208} + one nucleon. Some of the lowest one-phonon states. $\hbar\omega = 2.5$ MeV. Admixture: Squared amplitude.

Nucleus	J^π	Predominant configuration lj	NR	Main admixture %	$l'j'$	$N'R'$	Correction Δ MeV	Corrected energy $E+N\hbar\omega+\Delta$ MeV
Pb^{209}	9/2+	$g_{9/2}$	00	2	$g_{9/2}$	12	−0.11	−3.80
	11/2+	$i_{11/2}$	00	2	$i_{11/2}$	12	−0.11	−3.07
	5/2+	$d_{5/2}$	00	22	$g_{9/2}$	12	−0.42	−2.24
	15/2−	$j_{15/2}$	00	3	$j_{15/2}$	12	−0.07	−1.79
	1/2+	$s_{1/2}$	00	8	$d_{5/2}$	12	−0.27	−1.49
	7/2+	$g_{7/2}$	00[1]	55	$g_{9/2}$	12	−0.43	−1.10
	3/2+	$d_{3/2}$	00	4	$g_{7/2}$	12	−0.28	−0.88
	7/2+	$g_{9/2}$	12	37	$g_{7/2}$	00	−0.11	−1.3
	11/2+	$g_{9/2}$	12	0	—		0.00	−1.2
	9/2+	$g_{9/2}$	12	2	$g_{9/2}$	00	+0.06	−1.1
	5/2+	$g_{9/2}$	12	20	$d_{5/2}$	00	+0.29	−0.9
Bi^{209}	9/2−	$h_{9/2}$	00	2	$h_{9/2}$	12	−0.07	−3.61
	7/2−	$f_{7/2}$	00	2	$f_{7/2}$	12	−0.07	−2.76
	13/2+	$i_{13/2}$	00	2	$i_{13/2}$	12	−0.07	−2.34
	7/2−	$h_{9/2}$	12	0	—		+0.01	−1.0
	9/2−	$h_{9/2}$	12	2	$h_{9/2}$	00	+0.07	−1.0

[1] This configuration is not predominant, but is obtained in the limit when the coupling parameter e is 0.

more than one phonon. According to Bohr and Mottelson [9], the relevant matrix elements are given by[1]

$$\langle lj; 00; jM | H_{\text{int}} | l'j'; 12; jM \rangle = \mp \varepsilon \langle j | h | j' \rangle, \tag{10}$$

where $\varepsilon^2 = e \cdot \hbar\omega$, with $\hbar\omega$ = the phonon energy and $e = k^2/2C$ (k is the coupling constant and C the deformability). $\langle j | h | j' \rangle$ are real numbers, for which formulas are given in reference [9]. In all four cases we put $e = 0.69$ MeV, in agreement with an estimate by True and Ford [8] from the probability of the 0.57 MeV $E2$ transition in Pb^{207}. This value is probably of the right order of magnitude for nuclei adjacent to Pb^{208}. k is essentially constant, about 40 MeV [9]. C on the other hand, varies strongly and becomes large in the double-magic regions. The quantitative information is very incomplete in the lead region, but we assume C to have a value between 1000 and 1500 MeV, as has been found for Pb^{207} and Pb^{206} [8, 10].

The evidence for $\hbar\omega$ is also weak. The energy of the first excited 2^+ state for spherical even-even nuclei is known to increase rapidly as one moves towards closed shells (reference [10], especially Fig. V.3). In Pb^{208}, no 2^+ state has been found, but there is no strong evidence against it above 2.5 MeV [8]. One might expect that $\hbar\omega$ is of the order of 2 MeV for the nuclei $Pb^{208} \pm$ one nucleon. We will use $\hbar\omega = 1.5$ MeV

---

[1] − for particle, + for hole.

Table 5b. Collective corrections to the single-particle states in the cases Pb^{208} – one nucleon. Some of the lowest one-phonon states. $\hbar\omega = 1.5$ MeV. Admixture: Squared amplitude.

Nucleus	J^{π}	Predominant configuration		Main admixture			Correction Δ MeV	Corrected energy $E+\delta-N\hbar\omega+\Delta$ MeV
		lj	NR	%	$l'j'$	$N'R'$		
Pb^{207}	1/2−	$p_{1/2}$	00	4	$f_{5/2}$	12	+0.16	−7.24
	5/2−	$f_{5/2}$	00	10	$p_{1/2}$	12	+0.21	−8.08
	3/2−	$p_{3/2}$	00	15	$p_{1/2}$	12	+0.25	−8.22
	13/2+	$i_{13/2}$	00	4	$i_{13/2}$	12	+0.06	−8.94
	7/2−	$f_{7/2}$	00	14	$p_{3/2}$	12	−0.07	−10.75
	9/2−	$h_{9/2}$	00	5	$f_{5/2}$	12	−0.00	−11.29
	5/2−	$p_{1/2}$	12	9	$f_{5/2}$	00	−0.09	−9.0
	3/2−	$p_{1/2}$	12	13	$p_{3/2}$	00	−0.11	−9.0
	9/2−	$f_{5/2}$	12	5	$h_{9/2}$	00	+0.08	−9.7
	7/2−	$f_{5/2}$	12	16	$p_{3/2}$	12	+0.03	−9.8
	1/2−	$f_{5/2}$	12	17	$p_{3/2}$	12	−0.06	−9.9
Tl^{207}	1/2+	$s_{1/2}$	00	4	$d_{3/2}$	12	+0.15	−7.35
	3/2+	$d_{3/2}$	00	4	$s_{1/2}$	12	+0.16	−7.65
	11/2−	$h_{11/2}$	00	4	$h_{11/2}$	12	+0.06	−9.19
	5/2+	$d_{5/2}$	00	9	$s_{1/2}$	12	−0.07	−9.84
	7/2+	$g_{7/2}$	00	15	$d_{5/2}$	12	−0.03	−11.53
	5/2+	$s_{1/2}$	12	12	$d_{5/2}$	00	+0.11	−8.9
	3/2+	$s_{1/2}$	12	4	$d_{3/2}$	12	−0.05	−9.1
	7/2+	$d_{3/2}$	12	2	$g_{7/2}$	00	+0.05	−9.3
	1/2+	$d_{3/2}$	12	4	$s_{1/2}$	00	−0.08	−9.4

for Pb^{207} and Tl^{207}, and $\hbar\omega = 2.5$ MeV for Pb^{209} and Bi^{209}. The former choice is made on the following grounds. With reasonable values of the potential parameters, the $f_{7/2}$ neutron hole level in Pb^{207} always comes out 0.5–1.0 MeV higher in energy than the experimental $7/2^-$ level at 2.35 MeV (cf. reference [6]). We suggest that the latter is mainly an $f_{5/2}$ + one phonon state. This assumption, which will be discussed later, then fixes the value of $\hbar\omega$.

The calculation of the collective energy corrections Δ is performed by a straightforward diagonalization of the energy matrix, where the non-diagonal matrix elements are given by (10) (if not zero), and the diagonal ones are $E + N\hbar\omega$ for the particle cases, and $E + \delta - N\hbar\omega$ for the hole cases. This procedure also gives the perturbed wave functions. The results are given in Tables 5a and 5b, where we have also included some of the lowest perturbed one-phonon states.

A survey of experimental data for the nuclei Pb^{209}, Bi^{209}, Pb^{207}, and Tl^{207} is given in Appendix C. The theoretical and experimental energies are compared in Figures 2a and 2b for neutron and proton states respectively. Those levels, which have been suggested to be of core-excited (c.e.) or octupole vibrational (o.v.) character, have no counterparts among the theoretical levels in Figs. 2a and 2b.

As far as level data are well-known, the agreement between the calculated and the experimental energies is satisfactory. This fact supports the consistency of the method. It may therefore be justified to go somewhat further in the interpretation of experimental data and to make some predictions.

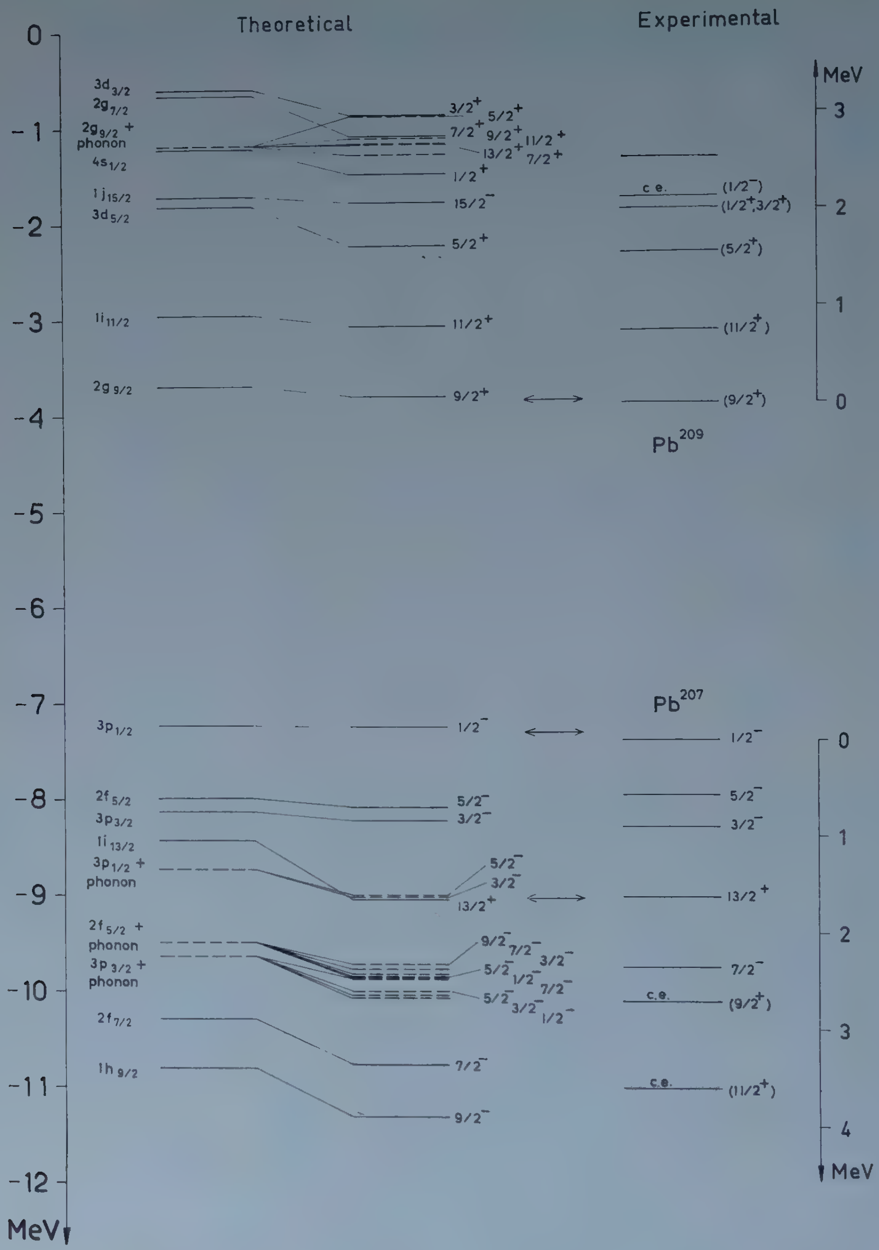

Fig. 2a. Theoretical unpertubed (to the left) and perturbed energies for neutron states, and experimental levels of the nuclei Pb^{208} ± one neutron. Dotted lines denote the lowest quadrupole vibrational states. Arrows indicate energies used for the choice of parameters. "c.e." means core-excited state.

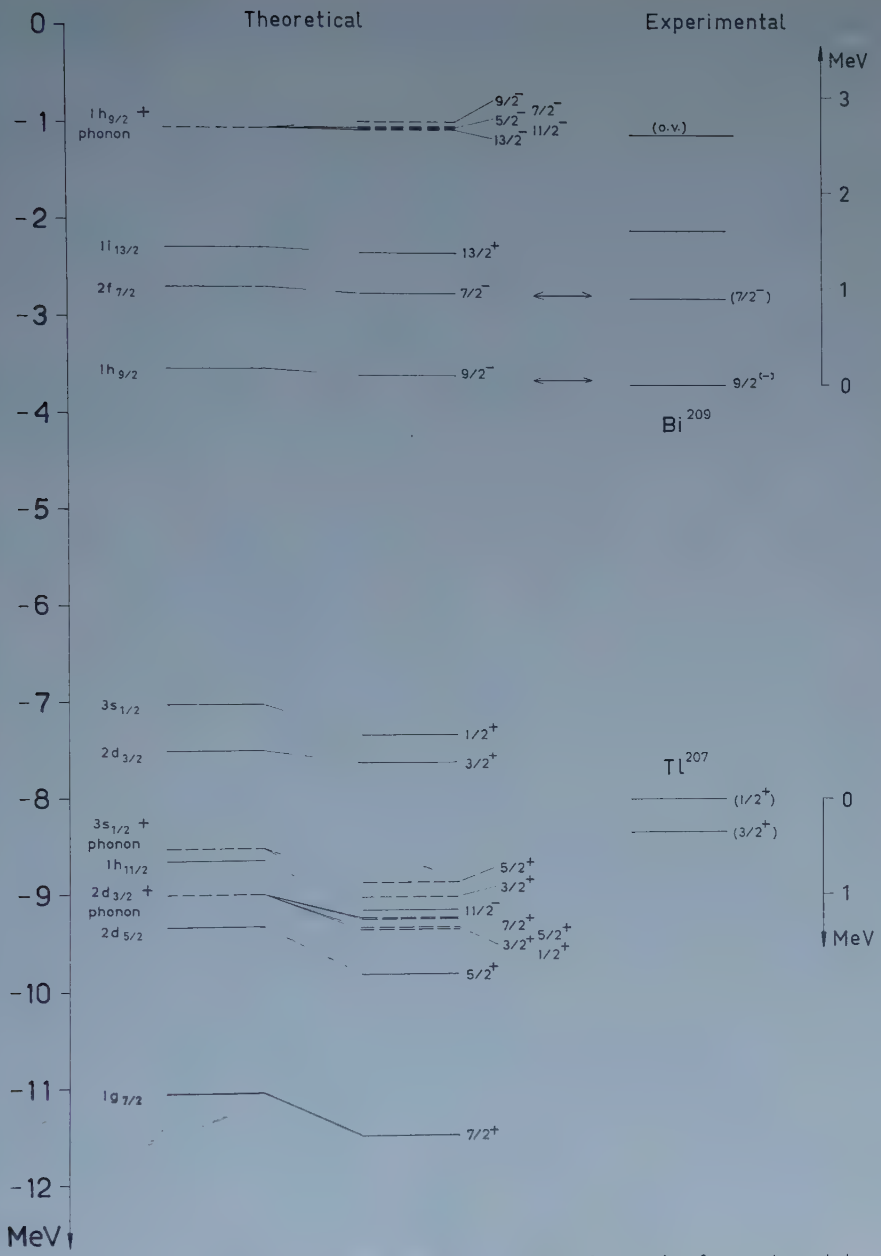

Fig. 2b. Theoretical unperturbed (to the left) and perturbed energies for proton states, and experimental levels of the nuclei Pb^{208} ± one proton. Dotted lines denote the lowest quadrupole vibrational states. Arrows indicate energies used for the choice of parameters. "o.v." means octupole vibrational state.

Pb^{209}.—The results support the assignments $9/2^+$, $11/2^+$ and $5/2^+$ for the three lowest states, as suggested by Harvey [11]. The $5/2^+$ level should have a fairly strong admixture of the vibrational $g_{9/2}$ + one phonon state (22 % with our choice of collective parameters).

The isomeric 2.13 MeV level is probably a core-excited $(p_{1/2})^{-1}$ $(g_{9/2})^2$ state as suggested by Stephens [12]. The energy agrees well with the difference between the neutron binding energies for Pb^{208} and Pb^{210}, 2.14 MeV.

Our results point to an $s_{1/2}$ rather than a $d_{3/2}$ assignment for the 2.01 MeV level.[1] The energy of the theoretical $s_{1/2}$ state could be lowered by using a potential form with a somewhat slower decrease for $r > R$.

Pb^{207}.—In choosing potential parameters, the positions of the $p_{1/2}$ and $i_{13/2}$ states have been adjusted to agree roughly with those of the corresponding experimental levels. The $f_{5/2}$ and $p_{3/2}$ states are seen to fit fairly well into the scheme.

The experimental $7/2^-$ level at 2.35 MeV should have mainly the structure of an $f_{5/2}$ neutron hole coupled to one phonon. There are two arguments which support this interpretation. In the first place, the 1.78 MeV γ-transition between the $7/2^-$ and $5/2^-$ states goes by ~ 94 % $E2$ and ~ 6 % $M1$ as deduced by Alburger and Sunyar [13] from a $\gamma-\gamma$ angular correlation measurement.[2] If this were a single neutron transition, one would expect the multipolarity $M1$ with a very small admixture of $E2$. Secondly, the 1.78 MeV transition is stronger than the 1.44 MeV transition to the $3/2^-$ level by a factor of 50, and hence the ratio between the reduced $E2$ transition probabilities is ~ 16. Both these facts indicate a collective $7/2^- \rightarrow 5/2^-$ transition.

The levels at 2.71 MeV and higher energies, which have been seen in the Pb^{206} (d,p) Pb^{207} reaction [11, 14], are probably core-excited states with a structure like the ground state of Pb^{206} with one neutron added in the next major shell. The $f_{7/2}$ and $h_{9/2}$ neutron hole states are not expected to show up in this reaction due to the small admixtures of $(f_{7/2})^{-2}$ and $(h_{9/2})^{-2}$ in the Pb^{206} ground state.

The possible vibrational $5/2^-$ and $3/2^-$ states occurring at an excitation energy of ~ 1.7 MeV would not be populated with sufficiently large intensities to be seen either in the (d,p) reaction or in the β decay of Bi^{207}.

The $9/2^-$ state from the coupling of an $f_{5/2}$ neutron hole to one phonon would be reached by electron capture from Bi^{207} with an intensity comparable to that of the $7/2^-$ state from the same configuration if it occurs at the same energy or lower. We have actually found the $9/2^-$ state to come somewhat lower than the $7/2^-$ state, but perturbations from states with two phonons may shift their order, as illustrated in intermediate coupling calculations by Choudhury [15]. The present experimental information does not exclude the existence of a $9/2^-$ state just above the $7/2^-$ state.

Bi^{209}.—For the first excited state, we have regarded the assignment $7/2^-$ as established. The theoretical results predict the assignment $i_{13/2}$ for the second excited state. The $p_{3/2}$, $f_{5/2}$, and $p_{1/2}$ states have been found to be unbound, but a potential form with a slower decrease for $r > R$ might bind the $p_{3/2}$ and $f_{5/2}$ states. Virtual single proton states should, for instance, give rise to low energy proton groups in the Pb^{208} (d,np) Pb^{208} reaction.

The experimental level (or levels) at 2.6 MeV, which is strongly excited in inelastic scattering of protons [16], may be interpreted, according to a suggestion by Lane, as an octupole vibrational state, being the counterpart of the first excited state in Pb^{208}. Alternatively, it can be considered as a core-excited state. Another possible interpretation might be that it belongs to the lowest group of quadrupole vibrational states.

---

[1] *Note added in proof:* This is also suggested by G. Holm, J. Burwell, and D. Miller from results of (d, p)-reactions on Pb^{208} and Bi^{209} (to be published in Phys. Rev.).

[2] *Note added in proof:* Predominant M1 character has, however, been obtained from polarization-direction measurements by P. H. Stelson, W. G. Smith, and F. K. McGowan (to be published in Phys. Rev.).

Tl^{207}.—The energy separation of the two lowest states is well reproduced by the theoretical results, and the suggested spin and parity assignments are confirmed. The absolute energies, however, disagree by about 0.7 MeV. The agreement can be considerably improved by changing the potential parameters for protons, while keeping them unchanged for neutrons, but this has not been done as the significance of such a procedure is doubtful.[1]

The $h_{11/2}$ state is expected to decay by an $M4$ transition to the $d_{3/2}$ state, unlike the lighter odd Tl-isotopes, for which the $h_{11/2}$ state should decay with multipolarity $E3$ to the experimentally observed $5/2^+$ state at 0.6–0.8 MeV [17]. Because of the small separation of this $5/2^+$ state and the $d_{3/2}$ state, the former can hardly be interpreted as $d_{5/2}$, but should rather be due to neutron excitation and should therefore not occur in Tl^{207}.

4. Discussion

For the potential terms (1), (2), (3) and the involved parameters we have made the following basic assumptions:

1. The nuclear potential $V(r)$ is a monotonic function, and its variation is symmetric around the point $r = R$.
2. The parameter V_0 is energy independent but has unequal values for neutrons and protons.
3. Except for the difference between V_0^p and V_0^n, the potential parameters are the same for the different nuclei.
4. The spin orbit term has the radial dependence $r^{-1} V'(r)$.
5. The Coulomb term is chosen to correspond to a uniform charge distribution.

The last assumption is not quite correct. One should rather use a charge density with a smooth decrease at the nuclear surface. The details of the charge distribution are, however, not crucial for the purpose of the present work. Assumption 4 is somewhat arbitrary but physically reasonable, and the results are not very sensitive to the radial dependence of the spin-orbit interaction, provided it is concentrated to the nuclear surface.

The condition 1 is fulfilled by the mathematically convenient form (1) of the diffuse potential. As mentioned above, one might in some cases get a better fit to the data by using a potential with a slight asymmetry around $r = R$. This could be achieved by "filling up" the function $V(r)$ in a suitable interval for $r > R$.

Assumption 2, about the energy independence of V_0, is not altogether satisfactory. From optical model analysis [3, 4], V_0 is found to decrease with increasing nucleon bombarding energies, and one might expect the same tendency to hold for bound states. This is also one of the results of Brueckner's theory of nuclear matter [18]. However, it seems as yet difficult to draw any definite conclusions about the magnitude of the variation of V_0 with energy for bound states in a nucleus. The main effect of the energy dependence would be to give, on the average, a larger spacing between the levels. It can also account for part of the difference between V_0^p and V_0^n. For a proton has, due to the Coulomb repulsion, a lower mean kinetic energy than a neutron with the same binding energy and therefore a larger value of V_0. The other part of the difference is probably to be explained by the facts that the effective nucleon-nucleon interaction is stronger between unlike than like nucleons, and that a proton has more neutrons to interact with than vice versa.

---

[1] This modification would also reduce the separation of the perturbed $d_{3/2}$ and $h_{11/2}$ levels to about 1.0 MeV, which indicates that we may have overestimated the energy difference between the $3/2^+$ and $11/2^-$ states.

The assumption 3 is to be regarded as part of the definition of the model applied in the present work. According to this, the nuclear mean potential represents the interaction of one nucleon with the residual nucleus, consisting of the spherical "core" of 126 neutrons and 82 protons. Thus the radius R has been kept at a constant value appropriate to $A = 208$, and the factor $Z-1$ in the Coulomb term (3) has been put equal to 82 for both the proton and the proton hole cases. Accordingly, no attempt has been made to trace a dependence of V_0, a, and λ on the individual nucleus, as has been done by Sliv and Volchok [6]. In this respect our approach is essentially different from theirs, as we apply corrections due to collective and pairing effects. Yet the nuclear parameters may have some individual variations, which we have neglected.

The justification for the choice of the collective parameters $\hbar\omega$ and e has been discussed above. The values of $\hbar\omega$ chosen for $A = 207$ and $A = 209$ are rather uncertain but not physically unreasonable. e may vary somewhat from nucleus to nucleus, but due to the lack of information we have put it constant, equal to the value obtained for Pb^{207}.

The choice of the parameter K in the expression (9) for the pairing energy may be subjected to criticism. Matrix elements for the short range forces used by True and Ford [8], in good agreement with experimental data for Pb^{206}, correspond to a value of K about twice as large as our choice. This comparison is, however, not very conclusive. If a larger K-value is assumed, one must also, to some extent, adjust the potential parameters. We have not entered upon this readjustment, particularly as it should not essentially influence the results or any conclusions drawn from them.

Finally one might discuss the conditions (I)–(III) for the choice of the potential parameters, especially concerning the use of the nucleon binding energies. However, the details of the assumptions are not very critical. The requirement (III), which may seem to be somewhat arbitrary, helps to fix the parameters V_0^n, V_0^p, and R and gives the approximately correct binding power of the nuclear potential. The separations of the levels within the major shells, on the other hand, furnish tests for the parameters a and λ. With the data available so far, it is probably not possible to determine the potential parameters in an essentially more consistent way.

In conclusion one would like to express the expectation that many new experiments will be done to investigate the properties of the low-lying levels of the nuclei Pb^{207}, Pb^{209}, Tl^{207}, and Bi^{209}. The experimental information is as yet generally too scanty to admit more detailed theoretical investigation along the present lines.

ACKNOWLEDGEMENTS

We would like to express our sincere thanks to the head of the Nobel Institute, Professor Manne Siegbahn, for his kind interest in our work. We are very much indebted to Laborator I. Bergström and Professor L. Hulthén for their valuable help and encouragement. Thanks are also due to several members of our institutes in Stockholm and of NORDITA and UITF in Copenhagen for enlightening discussions on various aspects of this work, and to fil. mag. Z. Sujkowski, who has performed some lengthy numerical calculations. Further, we gratefully acknowledge the free machine time at the computer BESK, granted by the Swedish Board for Computing Machinery.

The work has been economically sponsored by the State Council of Technical Research.

Nobel Institute of Physics, Stockholm, and Division of Mathematical Physics, Royal Institute of Technology, Stockholm, October 1959.

APPENDIX A

The wave function near $r = 0$

For $r \leqslant b \leqslant R$ one can, with sufficient accuracy, set

$$\xi(r) = 1 \quad \text{and} \quad \frac{1}{r}\,\xi'(r) = 0.$$

In the same interval, the function ζ_p in (3a) can also be given a non-essential change so that

$$\frac{\zeta_p(r)}{r} = \frac{3}{2R} = \text{constant}.$$

The equation then becomes, for $r \leqslant b$,

$$y''(r) + \left[\beta^2 - \frac{l(l+1)}{r^2}\right] y(r) = 0, \tag{A.1}$$

with

$$\beta = (\varkappa^2 - \varkappa_c^2 - k^2)^{1/2}. \tag{A.2}$$

$$\left.\begin{aligned} \varkappa^2 &= 0.04823\, V_0, \quad k^2 = 0.04823\,|E|, \\ \varkappa_c^2 &= 0.10409\,\frac{Z-1}{R} \quad (0 \text{ for neutrons}). \end{aligned}\right\} \tag{A.3}$$

The solution with $y(0) = 0$ is

$$y(r) = N_1 r^{1/2} J_{l+1/2}(\beta r), \tag{A.4}$$

where N_1 is a normalization constant. With the actual choice of b, the Bessel-function can be sufficiently well approximated by the first few terms of its series expansion in powers of βr. From this one can also easily calculate the logarithmic derivative of $y(r)$ at the point $r = b$, which is used in the numerical treatment of the eigenvalue problem.

The asymptotic form of the wave function

From a point $r = d$ and outwards, the function $\xi(r)$ and its derivative are negligible, and the wave equation thus reads, for $r \geqslant d$,

$$y''(r) - \left[k^2 + \frac{l(l+1)}{r^2} + \frac{2\eta k}{r}\right] y(r) = 0, \tag{A.5}$$

with k^2 according to (A.3) and η defined by

$$2\eta k = 0.06939\,(Z-1) \quad (0 \text{ for neutrons}).$$

The solution that asymptotically approaches zero is

$$y(r) = N_2 W(-\eta, l+1/2, 2kr),$$

N_2 being a normalization constant. W is the Whittaker function in ordinary notation. We use the integral representation

$$y(r) = N_2' e^{-kr-\eta \log 2kr} \int_0^\infty t^{l+\eta} \left(1 + \frac{t}{2kr}\right)^{l-\eta} e^{-t}\, dt. \tag{A.6}$$

A certain approximation method has been used for computing this function in the intervals of interest. In the case $\eta = 0$ (neutrons), the Whittaker function reduces to a Hankel function with imaginary argument. For $\eta > l$ there are special difficulties. However, it is possible in all the cases to compute the "tails" of the wave functions with sufficient accuracy for the present purposes.

APPENDIX B

The functions $y(r)$ according to (6),

$$y(r) = r R(r),$$

where $R(r)$ is the normalized radial wave function, are given in Tables B 1–B 3.

APPENDIX C

Experimental data

Of the four "single-particle nuclei", Pb^{207} is stable, Bi^{209} stable or nearly so, and Pb^{209} and Tl^{207} are β^--emitters. From the tables of Wapstra [19], one finds the neutron binding energies of Pb^{209} and Pb^{208} and the proton binding energies of Bi^{209} and Pb^{208} to be 3.87, 7.38, 3.72, and 8.05 MeV respectively. Experimental excitation energies, spins, parities, and decay properties of levels in the four nuclei are given in Table C 1. Assignments, which are considered tentative or not quite certain, have been put in parenthesis.

The experimental results for Pb^{209} are rather scanty. Some information has been obtained from (d,p)-reactions [11, 14], some from spectroscopical investigation [12]. The assignments are not known with certainty, not even for the ground state, although $9/2^+$ seems very probable.

Table B 1. The function $10^3 y(r)$ for neutron states.

r 10^{-13} cm	$3\,d_{3/2}$	$2\,g_{7/2}$	$4\,s_{1/2}$	$1\,j_{15/2}$	$3\,d_{5/2}$	$1\,i_{11/2}$	$2\,g_{9/2}$
0	0	0	0		0		0
0.5	8	0	209		9		0
1	57	2	315		61	0	2
1.5	159	16	265	0	169	1	15
2	281	57	85	1	301	4	52
2.5	361	138	−138	4	393	15	128
3	343	256	−293	15	383	44	243
3.5	208	380	−303	42	247	102	372
4	−6	461	−164	96	21	196	472
4.5	−217	451	56	183	−213	321	492
5	−335	324	248	303	−358	456	399
5.5	−309	102	321	437	−352	567	199
6	−152	−151	243	555	−197	618	−59
6.5	68	−359	56	619	39	594	−300
7	266	−472	−156	606	262	509	−455
7.5	388	−489	−318	525	405	396	−500
8	433	−445	−403	410	454	289	−461
8.5	426	−377	−424	298	438	204	−382
9	393	−309	−409	209	392	142	−299
9.5	352	−250	−377	144	337	99	−228
10	312	−202	−340	99	286	69	−172
10.5	275	−164	−304	69	240	49	−130
11	242	−133	−271	48	201	35	−98
11.5	214	−109	−240	34	169	25	−74
12	189	−90	−213	25	142	18	−56
12.5	167	−74	−189	18	119	13	−43
13	148	−62	−167	13	101	10	−33
13.5	132	−52	−148	10	85	7	−25
14	117	−44	−131	7	72	5	−20
14.5	105	−37	−116	5	61	4	−15
15	93	−31	−103	4	51	3	−12
15.5	84	−27	−91	3	43	2	−9
16	75	−23	−81	2	37	2	−7
16.5	67	−19	−71	2	31	1	−6
17	61	−17	−63	1	27	1	−4
17.5	54	−14	−56	1	23	1	−3
18	49	−12	−50	1	19	1	−3
18.5	44	−11	−44	1	16	1	−2
19	40	−9	−39	1	14	0	−2
19.5	36	−8	−35	0	12		−1
20	32	−7	−31		10		−1
20.5	29	−6	−27		9		−1
21	26	−5	−24		7		−1
21.5	24	−5	−21		6		−1
22	22	−4	−19		5		0
22.5	20	−4	−17		5		
23	18	−3	−15		4		
23.5	16	−3	−13		3		
24	15	−3	−12		3		
24.5	13	−2	−10		3		
25	12	−2	−9		2		

Table B 2. The function $10^3 y(r)$ for neutron hole states.

r 10^{-13} cm	$3\,p_{1/2}$	$2\,f_{5/2}$	$3\,p_{3/2}$	$1\,i_{13/2}$	$2\,f_{7/2}$	$1\,h_{9/2}$
0	0	0	0		0	
0.5	58	1	58		1	
1	204	11	201		10	0
1.5	359	51	358	0	46	2
2	438	135	441	2	123	10
2.5	383	259	394	10	240	31
3	194	393	213	30	373	78
3.5	−67	488	−44	73	479	157
4	−301	493	−285	147	508	269
4.5	−417	383	−416	253	430	400
5	−367	170	−384	380	246	522
5.5	−172	−92	−204	506	−4	602
6	89	−327	54	595	−253	616
6.5	320	−472	294	621	−432	559
7	453	−508	442	572	−504	453
7.5	477	−457	477	469	−476	334
8	428	−369	432	347	−391	230
8.5	350	−278	353	240	−293	152
9	272	−202	272	159	−209	98
9.5	206	−145	203	103	−146	63
10	154	−103	150	67	−100	41
10.5	115	−73	109	44	−68	26
11	85	−52	80	29	−47	17
11.5	63	−37	58	19	−32	11
12	47	−26	42	12	−22	7
12.5	35	−19	31	8	−15	5
13	26	−13	23	6	−10	3
13.5	19	−10	16	4	−7	2
14	14	−7	11	3	−5	1
14.5	11	−5	8	2	−3	1
15	8	−4	6	1	−2	1
15.5	6	−3	4	1	−2	0
16	4	−2	3	1	−1	
16.5	3	−1	2	0	−1	
17	2	−1	2		−1	
17.5	2	−1	1		0	
18	1	−1	1			
18.5	1	0	1			
19	1		1			
19.5	1		0			
20	0					

The positions of some low-lying states of Bi^{209} are well established by various experiments, mainly inelastic nucleon scattering [16, 20]. The ground state spin is known from atomic spectroscopy to be 9/2.

In Pb^{207} four excited states below 2.5 MeV are well-known from spectroscopical investigations of the decay of Bi^{207}, especially the work by Alburger and Sunyar [13]. Harvey [11] obtains from (d,p)- and (d,t)-reactions all the states given in Table C 1, and also further states up to 5 MeV. More recent verifications are furnished by the results from the (d,p)-reactions of McEllistrem *et al.* [14] and the (p,p')-reactions of Cohen and Rubin [16]. Atomic spectroscopy gives the spin 1/2 of the ground state.

Table B 3. The function $10^3\, y(r)$ in the proton cases.

r 10^{-13} cm	Proton states			Proton hole states				
	$1\, i_{13/2}$	$2\, f_{7/2}$	$1\, h_{9/2}$	$3\, s_{1/2}$	$2\, d_{3/2}$	$1\, h_{11/2}$	$2\, d_{5/2}$	$1\, g_{7/2}$
0		0		0	0		0	0
0.5		1		251	6		5	0
1		10	0	421	44	0	40	1
1.5	0	45	2	455	131	1	121	6
2	2	122	10	341	261	6	243	22
2.5	10	240	32	115	400	22	379	61
3	30	378	80	−149	502	56	488	129
3.5	73	490	162	−363	519	118	524	230
4	148	526	279	−453	425	213	458	354
4.5	258	450	416	−388	226	334	289	482
5	393	258	543	−189	−32	464	47	582
5.5	524	−6	622	76	−281	573	−206	624
6	616	−268	626	316	−453	627	−404	595
6.5	634	−450	552	457	−511	607	−498	500
7	570	−510	430	478	−464	515	−482	373
7.5	449	−463	301	408	−361	386	−392	250
8	316	−361	195	304	−252	259	−280	155
8.5	205	−256	121	208	−165	161	−184	92
9	127	−172	74	136	−104	95	−115	50
9.5	77	−113	45	87	−64	55	−70	30
10	47	−74	27	55	−40	32	−43	17
10.5	29	−48	17	35	−25	19	−26	10
11	18	−32	10	22	−15	11	−16	6
11.5	11	−21	7	14	−10	6	−10	3
12	7	−14	4	9	−6	4	−6	2
12.5	5	−9	3	6	−4	2	−4	1
13	3	−6	2	4	−2	1	−2	1
13.5	2	−4	1	2	−2	1	−1	0
14	1	−3	1	2	−1	1	−1	
14.5	1	−2	1	1	−1	0	−1	
15	1	−1	0	1	0		0	
15.5	0	−1		0				
16		−1						
16.5		−1						
17		0						

The information about Tl^{207} is very meagre, and only one γ-ray has been attributed to that nucleus [21], supplementing the information from α-spectroscopy. Systematics of odd Tl isotopes indicate the ground state spin 1/2. Cf. Bergström and Andersson [17].

Concerning the ground state moments of the four nuclei, the situation is briefly the following. For Pb^{209} and Tl^{207} nothing is known experimentally. The magnetic moment of Bi^{209} is $+4.1$ nuclear magnetons, and the deviation from the Schmidt value $+2.6$ has been attributed to configuration mixing. For Pb^{207} the experimental value agrees with the Schmidt value, $+0.6$ nuclear magnetons. The quadrupole moment of Bi^{209} is -0.3 (in units of $e \cdot 10^{-24}$ cm²), and the shell model value is -0.2. A possible difference may be ascribed to weak surface coupling, but gives no significant information about the collective parameters.

Table C1. Experimental level data.

	Energy MeV	J^{π}	Decay properties
Pb^{209}	0	$(9/2^+)$	β^-
	0.75	$(11/2^+)$	
	1.56	$(5/2^+)$	1.56 MeV, γ
	2.01	$(1/2^+, 3/2^+)$	0.45 MeV, γ
	2.13	$(1/2^-)$	3 $m\mu$ sec, 0.12 MeV, γ $(E1)$
	2.54		
Bi^{209}	0	$9/2^-$	Stable (or α)
	0.90	$(7/2^-)$	0.90 MeV, $M1$
	1.61		1.61 MeV, γ
	2.60		
Pb^{207}	0	$1/2^-$	Stable
	0.570	$5/2^-$	0.1 mμ sec, 0.570 MeV, $E2$
	0.90	$3/2^-$	0.90 MeV, γ
	1.634	$13/2^+$	0.8 sec, 1.064 MeV, $M4$
	2.35	$7/2^-$	1.78 MeV, $E2$ ($\sim 94\%$) + $M1$ ($\sim 6\%$); 1.45 MeV, γ
	2.71	$(9/2^+)$	
	3.61	$(11/2^+)$	
Tl^{207}	0	$(1/2^+)$	β^-
	0.350	$(3/2^+)$	0.350 MeV, $M1 + E2$

REFERENCES

1. J. P. Elliott and A. M. Lane, Handbuch der Physik, Vol. *39*, p. 241. (Springer 1957.)
2. R. D. Woods and D. S. Saxon, Phys. Rev. *95*, 577 (1954).
3. S. Fernbach, Rev. Mod. Phys. *30*, 414 (1958).
   H. H. Barschall, Comptes Rendus du Congrès International de Physique Nucléaire, p. 7. (Dunod, Paris 1959.)
4. A. E. Glassgold, Rev. Mod. Phys. *30*, 419 (1958).
   A. E. Glassgold, Comptes Rendus du Congrès International de Physique Nucléaire, p. 23. (Dunod, Paris 1959.)
5. A. A. Ross, H. Mark, and R. D. Lawson, Phys. Rev. *102*, 1613 (1956).
6. L. A. Sliv and B. A. Volchok, J. Exp. Theor. Phys. *36*, 539 (1959).
7. K. Bleuler and C. Terreaux, Helv. Phys. Acta *30*, 183 (1957).
   A. Schröder, Nuovo Cimento *7*, 461 (1958).
8. W. W. True and K. W. Ford, Phys. Rev. *109*, 1675 (1958).
9. A. Bohr and B. R. Mottelson, Dan. Mat. Fys. Medd. *27*, no. 16 (1953).
10. K. Alder *et al.*, Rev. Mod. Phys. *28*, 432 (1956).
11. J. A. Harvey, Can. J. Phys. *31*, 278 (1953).
12. D. Strominger, F. S. Stephens Jr., and J. O. Rasmussen, Phys. Rev. *103*, 748 (1956).
13. D. E. Alburger and A. W. Sunyar, Phys. Rev. *99*, 695 (1955).
14. M. T. McEllistrem, H. J. Martin, D. W. Miller, and M. B. Sampson, Phys. Rev. *111*, 1636 (1958).
15. D. C. Choudhury, Dan. Mat. Fys. Medd. *28*, no. 4 (1954).
16. B. L. Cohen and A. G. Rubin, Phys. Rev. *111*, 1568 (1958).
17. I. Bergström and G. Andersson, Arkiv Fysik *12*, 415 (1957).
18. K. A. Brueckner and J. L. Gammel, Phys. Rev. *109*, 1023 (1958).
19. A. H. Wapstra, Handbuch der Physik, Vol. *38*, p. 1. (Springer 1958.)
20. M. A. Rothman and C. E. Mandeville, Phys. Rev. *93*, 796 (1954).
    R. M. Kiehn and C. Goodman, Phys. Rev. *95*, 989 (1954).
    R. B. Day, Phys. Rev. *102*, 767 (1956).
    F. I. Boley, E. H. Thorndike, and A. T. Moffet, Phys. Rev. *110*, 915 (1958).
21. P. Falk-Vairant, J. Teillac et C. Victor, J. Phys. Radium, *13*, 313 (1952).

Tryckt den 25 februari 1960

Uppsala 1960. Almqvist & Wiksells Boktryckeri AB